Co-granulation of low rates of graphene and graphene oxide with macronutrient fertilizers remarkably improves their physical properties

Shervin Kabiri [ǂ], *Roslyn Baird*[ǂ], *Diana N.H. Tran*[ǂ], *Ivan Andelkovic*[ǂǂ], *Mike J. McLaughlin**[ǂ]*and Dusan Losic** [ǂ]

[ǂ] School of Chemical Engineering, Engineering North Building, The University of Adelaide, Adelaide, SA 5005, Australia

[ǂǂ] Fertilizer Technology Research Centre, School of Agriculture, Food and Wine, The University of Adelaide, Waite Campus, PMB1, Glen Osmond, SA 5064, Australia

Email addresses of Authors:

Shervin.kabiri@adelaide.edu.aau

Roslyn.baird@adelaide.edu.au

Diana.tran@adelaide.edu.au

Ivan.andelkovic@adelaide.edu.au

michael.mclaughlin@adelaide.edu.au

dusan.losic@adelaide.edu.au

Keywords: Graphene, Graphene oxide, Fertilizers, Crushing strength, Abrasion, Impact resistance, Caking tendency

ABSTRACT

The beneficial effects of graphene (GN) and graphene oxide (GO) additives on the physical properties of monoammonium phosphate (MAP) fertiliser granules were investigated. Low doses (0.05 to 0.5% w/w) of GN and GO sheets were co-granulated with MAP and effects on the crushing strength, abrasion and impact resistance of prepared granules were evaluated. Co-granulation with 0.5% w/w GN sheets (MAP-GN) significantly enhanced the mechanical strength of MAP granules (~18 times improvement) while inclusion of same amounts of GO sheets (MAP-GO) improved the strength to a lesser extent (~8 times improvement). The co-granulation of GN also improved MAP granules resistance to abrasion (>70 %) and impact resistance (>75 %). Heating MAP-GO granules at 50°C after granulation is shown to enhance their physical properties in comparison to MAP-GO granules dried under ambient temperatures. The advantages of GN and GO sheets compared with current additives in enhancing the physical properties of MAP granules are

explained by their high specific area, superior nanofiller-matrix and adhesion/interlocking ability arising from their unique wrinkled structures and two-dimensional (2D) geometry. These results confirm the potential of GN/GO additives to enhance the physical properties of MAP granules that could be translated to other fertilizers and applied in the industry.

INTRODUCTION

Fertilizers are common amendments to agricultural soils to refill the soil during the harvest with plant essential nutrients and improve crop yields and health for food production.[1, 2] One of the critical parameter in selection of particulate fertilizer is its physical quality. The acceptability of the fertilizers in the market not only is determined by their nutrient content but also by their physical quality and is often the reason for selecting one fertilizer over another.[3, 4] Also granular fertilizers should have appropriate mechanical strength to resist significant fracturing and creation of excessive dust during the handling and storage process to meet the needs of market.[5] However, most of the fertilizers produced by different techniques such as granulation, prilling or compaction techniques are never perfectly spherical and suffer from having irregular protrusions on their surface.[4] These protrusions and jagged edges tend to weaken and break off during the routine handling of fertilizers, or transport and spreading on the farm and create substantial quantities of dust.[4, 6] This airborne dust produced is undesirable due to its health and safety risks for those exposed during manufacturing of fertilizers or their application on the farm. Furthermore, the abrasion of granules and dust formation leads to negative environmental impacts and increased costs for both fertiliser producers and users due to the loss of nutrient.[4]

Another issue associated with handling of fertilizer granules is their tendency to cake during bulk storage and transportation as the initial free-flowing particles may absorb water and form a solid agglomerated coherent mass.[7-9] This can be the result of crystal bridges formed between granules as the air humidity cycles, dissolving the surfaces causing recrystallization to occur.[8] The caked particles may easily break into smaller particles producing significant amounts of dust during handling and transporting or hard agglomerates may block the spreading equipment resulting in uneven nutrient spreading when applied to the soil. [9, 10]

To overcome these considerable drawbacks manufacturers use different hardening additives or coating materials to improve the physical properties of fertilisers and reduce the propensity for dust generation and caking. For example, anti-dusting properties have been imparted to urea fertilizers by utilizing formaldehyde or low concentrations of lignosulfonate.[10-12] However, these additives have several disadvantages, formaldehyde use presents serious health and safety issues, whereas, lignosulfonate can discolour the urea product and affect acceptance in the marketplace.[10, 11] Addition of gelling type clay, such as attapulgite or sepiolite, to the urea melt or synthetic liquor has been used to overcome the previously discussed disadvantages and to increase the hardness of urea fertilizers. However, these mineral additives are needed in higher quantity to enhance the physical quality of fertilizer and their mining sites are located

in a geographical isolated area, therefore, the overall cost of the final product will increase.[11] Another strategy used to harden granules is to add a binder such as melamine and its hydrolysed products to bind fine particles of a poorly or slightly soluble source to form a hardened agglomerate or prill.[13] However, this method is restricted to nitrogen source materials with a certain size, and the granulation or prilling machinery used to make such hardened granular fertilizers are relatively expensive.[4] Calcium oxide, calcium hydroxide, cement and fly ash have also been used to improve the hardness of fertilizers especially urea. The problem with using these materials is the reduction of available fertilizer nutrient in the final granules.[11, 14]

Another approach to improve the physical properties and release performances of fertilizers is to coat fertilizer granules with different coating materials. Many materials have been considered for this purpose including molten elemental sulphur, diatomaceous earth and clay, hydrated cement, gypsum, zeolite, wax, plastic, and a combination of a biodegradable aliphatic co-polyester and fatty acids to create slow-releasing urea fertilizers that also have anti-caking properties.[15-18] Although these coatings decrease the rate of release of nutrients and in some cases enhance the anti-caking properties of the granules, most of them incorporate foreign elements into the fertilizers, which are not compatible with the specific fertilizer and sophisticated equipment is usually needed to apply them.[4, 14] In addition, coatings or materials that comprise a high percentage of the total fertilizer composition tend to dilute the available fertilizer nutrient content and increase transport and handling costs. Therefore, there is a need for new materials to address the limitations of currently used methods in terms of improved performance, multiple modes of action, very low dosages, and acceptable costs that can be used on an industrial scale.

Graphene (GN) and its oxidised form graphene oxide (GO) are new materials with unique properties, such as distinctive 2D structures, high surface area, tailorable surface chemistry and have exceptional mechanical properties.[19, 20] In fact, GN possesses a very high specific surface area with a theoretical value of 2630 m^2g^{-1}, since every atom of the single-layer sheet is exposed from both sides.[21, 22] Furthermore, despite being one atom thick, GN is the strongest material measured with a Young's Modulus of E=1.0 TPa and an intrinsic strength of 130 GPa in its pristine, atomically perfect form.[20] Therefore, these outstanding mechanical properties of GN have initiated considerable interest for their application as an additive to enhance the mechanical properties of softer materials and strengthen them. Most significant examples are the use of GN as nanofillers to increase the mechanical properties of different polymers due to the improved interactions of GN and the polymer matrix, resulting from the high surface area of the planar GN sheets.[23, 24] Two dimensional GN sheets are not only used as an ideal filler or reinforcing nanomaterial for polymer matrices, but are also incorporated on metal matrices or ceramics to enhance the properties of metal-matrix-composites or ceramic composites.[25-27]

GO is an oxidised form and water-soluble derivative of GN, with a high specific area, ultra-high strength, exceptional mechanical properties and flexibility.[19, 28] The hydrophilic nature of GO allows for a wide variety of chemical functionalization and provides stronger interactions with host materials.[22, 29] It has

been reported that GO has the capability of forming composites with polymers, construction materials and ceramics, and can remarkably enhance the toughness of formed composites by controlling the microstructure of crystals in the composites.[30 31, 32] Recent studies show that low dosages of GO (0.01-1 %) could significantly enhance the performance and mechanical properties of cement composites.[30, 33-36] GO can accelerate the hydration of cement due to its high surface area and also densify the cement microstructure as a filler because of the nano size and flexibility of the GO sheets.[33, 37]

Inspired by the unique properties of graphene-based materials (GBMs) and their capability to significantly improve the mechanical properties of many other composite materials with very low dosages, we proposed that these materials can be used as additives to enhance the physical properties of granular fertilizers. The aim of this work is to demonstrate that GN based additives in small quantities can significantly enhance the physical properties of commercial fertilizers and address the long standing problems caused by their fragility and physical losses related to low crushing strength, abrasion and impact resistance. Monoammonium phosphate (MAP) was used as a model to demonstrate this concept, as it is a widely used fertilizer that is transported and handled around the globe and could be prepared in the laboratory. GN and GO materials were made from low cost natural graphite using scalable industry processes and their co-granulation into MAP granules were performed using a rotating pan and water atomization process commonly used in the fertilizers industry. The addition of both GN and GO additives were explored using different dosages (0.05 to 0.5% w/w) to investigate their effect on improving the key physical properties of MAP granules including the crushing strength, abrasion, impact resistance and caking tendency of granules and compared with MAP (no additive). Finally to demonstrate the additional benefits of these additives on MAP granules the release of nutrients from GN and GO treated granules was evaluated in soil.

EXPERIMENTAL SECTION

Synthesis of GO and GN. GO sheets were synthesised by the improved Hummer's method from graphite powders.[38] A modified hydrothermal method for the reduction of GO was used to prepare the GN sheets. [39] A GO dispersion (1 mg ml^{-1}, 500 ml) was transferred to a Teflon lined autoclave and heated at 180°C for 2 h. The autoclave was then cooled to room temperature and the formed GN hydrogel was ultrasonicated in a H_2O/acetone (ratio 3:1) mixture. Some of the final product was freeze-dried for FTIR, Raman, XRD, TGA and SEM characterization and particle size measurement. (Figure S1and S2, Supporting Information).

Preparation of monoammonium phosphate (MAP) fertilizer granules co-granulated with GN (MAP-GN) and GO (MAP-GO). Monoammonium phosphate granules were ground and sieved to obtain a powder with sizes less than 250 µm. A GN or GO paste with ~20% water was mixed with the MAP powder at dosage rates of 0.05%, 0.1%, 0.2% and 0.5% by weight. GN and GO sheets with particle sizes of ~150 and ~200 µm, respectively, were added in wet form to reduce the risk of dust exposure during formulation. The mixtures of MAP with different ratios of GN or GO were homogenised, dried and sieved through a 250 µm sieve before granulation. The MAP fertilizer mixture with GN or GO (3 g) were placed in a rotating pan and a small amount of ultrapure deionised water was sprayed onto the fertilizer using a 50 µl min^{-1} nebulizer while the drum was rotating at 12-15 rpm at an angle of 39.2 Deg. The fertilizer powder was granulated in the rotating pan to form particles of approximately 2-4 mm in size, separated by sieving. Oversize granules were crushed and re-granulated.

Granule crushing strength. To measure crushing strength, fertilizer samples were screened according to International Fertilizer development Centre (IFDC) method S-107 to obtain at least 25 granules with sizes between 2.80 and 2.36 mm diameter.[40] A commercial table-top Wykeham Farrance ring penetrometer (England) was used to measure the mechanical strength of the fertilizer granules. Individual granules were placed on a mounted flat surface and pressure was applied by a flat-end rod attached to the compressor tester. A gauge mounted in the compression tester measured the pressure required to fracture the granule. The load at which the granule fractured was considered as the crushing strength and a total of 25-30 parallel measurements were carried out for each formulation. The average of those measurements determined the crushing strength of the granules.

Granule abrasion test. Abrasion resistance of granules was measured by modifying IFDC S-116.[40] To measure the abrasion resistance of the MAP fertilizers, first the samples were screened over 2.80- and 1.00-mm sieves. A portion of the fertilizers (50 g) was accurately weighed and placed in a container. The container was placed in a Spex-mixer/Mill (8000M Mixer/Mill) and rotated at 30 rpm for times ranging between 5 to 30 seconds and 5 minutes. The contents were removed and hand screened over a 1.0 mm screen for 5 minutes. The material retained on the 1.0 mm screen was then weighed and the ''percentage of degradation'' was calculated as follows:

$$degradation\ \% = 100 - 100 \times \frac{Wt\ of -2.80{+}1.00\ mm\ fraction\ recovered}{Wt\ of -2.80{+}1.00\ mm\ fraction\ charged} \quad (1)$$

Granule impact resistance. Impact resistance of granules was measured by modifying IFDC method S-118.[40] Each fertilizer formulation (200 g) was passed through a series of sieves; namely 2.80mm, 2.36mm and 2.00 mm. The size range of granules selected for testing in this case was between 2.00 mm and 2.80 mm diameter which contained 85% of the overall sample. The 100 g (±1 g) subsamples were accurately weighed and then allowed to fall 10.7 m in an 15cm diameter enclosed pipe and impact on a metal catch plate in a catch pan at the base of the pipe. The dropped samples were collected and screened over the smallest selected sieve. The material retained on the previously selected sieve was weighed and the percentage of ''shattered granules'' was calculated as follow:

$$shattered\ granules\ \% = 100 - 100 \times \frac{material\ retained\ on\ bottom\ sieve\ after\ test\ (g)}{100\ g\ (\pm 1)} \quad (2)$$

Caking tendency of fertilizer granules. To investigate the caking tendency of the fertilizers an apparatus was made similar to the caking apparatus designed by Lafci et al.[41] The apparatus consisted of a PVC cylindrical mould and a plunger. The internal diameter of the cylindrical mould was 2 cm and its height was 7 cm. The mould can be split into two parts so that the cake formed could be removed without any breakage. To study the influence of pressure on caking 4.0 g of MAP-0.5%GN, MAP-0.5%GO and untreated MAP formulations were placed in each caking apparatus and loads applied from 1 kg to 2.5 kg using weights placed on the plunger. All caking tendency experiments were conducted in a humidity chamber (Environmental Temperature and Humidity Cabinets, Envirotherm,Thermoline Scientific, Australia) with 70% humidity (near to the critical relative humidity of MAP fertilizers) at 30 ºC. Samples were taken at the end of 7 days from the humidity chamber and where any cakes were formed the force needed to crush them were determined using a ring penetrometer.

Phosphorus (P) diffusion from fertilizer granules. The P diffusion method of Degryse and McLaughlin was used to investigate the release of P from amended and untreated MAP granules.[42] Briefly, Petri dishes with a diameter of 5.5 cm and 1 cm height were filled with wetted soil and a granule of the selected products (MAP-0.05%GN, MAP-0.5%GN, MAP-0.05%GO, MAP-0.5%GO and MAP) were placed in the centre of the Petri dish at the same dosage rate (~6.3 mg per Petri dish) about 4 mm below the soil surface. Three replicates were prepared for each formulation. The Petri dishes were then placed in a plastic bag with moist paper towels to avoid water loss from the soil and incubated at 25°C. The release and diffusion of P from the granules was monitored at 1, 3, 14, 21 and 28 days.

RESULTS AND DISCUSSION

Structural and chemical characterization of MAP granular fertilizer with GN and GO additives

Light and SEM microscopic images of prepared MAP samples (control and with GO/GN additives) showed that all samples were granulated to form round-shaped granules (Figure 1a-f). However,

the MAP granule (control) had a rougher surface compared to the MAP-GN and MAP-GO granule surfaces (Figure 1d-f). In order to confirm the presence and distribution of GN and GO sheets in the MAP-co-granules, higher magnification SEM images was taken and compared with MAP (Figure 1g-i). These images show GN (or GO) sheets randomly dispersed and embedded in the MAP-GN or MAP-GO composites where some of the MAP macroparticles were wrapped by the GN or GO sheets.

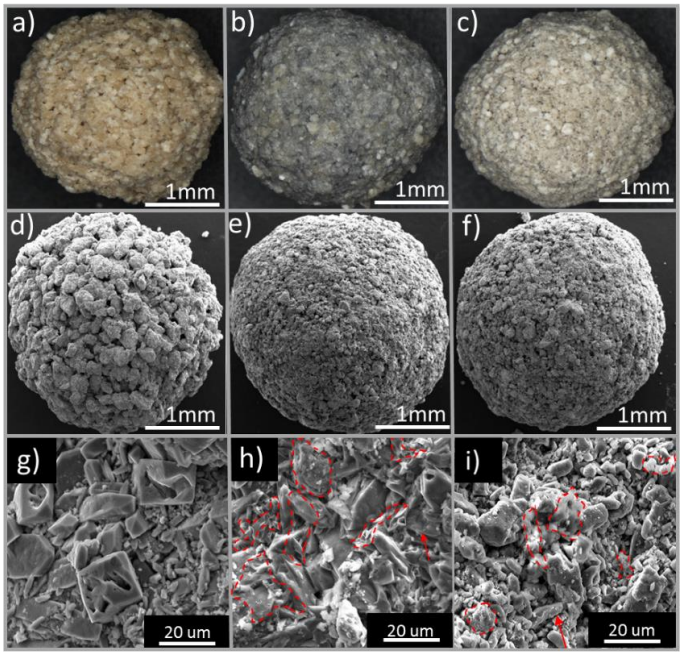

Figure 1. Microscopic images of a) Mono ammonium phosphate granules (MAP) (control), MAP with b) 0.5% graphene (GN) and c) 0.5% graphene oxide (GO), SEM images of d) MAP, MAP with e) 0.5% GN and f) 0.5% GO and high resolution SEM images of g) MAP, MAP with h) 0.5% GN and i) 0.5% GO. (Red arrows and dot points represent the presence of GN or GO).

The XRD patterns of GN and GO show typical diffraction peaks at $2\theta=25.1°$ (d-spacing ~0.35 nm) and $2\theta=9.9°$ (d-spacing ~0.90), respectively, compared to the XRD pattern of commercial MAP which can be indexed to the presence of $NH_4H_2PO_4$ (JCPDS card No. 9007583) (Figure 2a-b).[38, 43] Samples prepared with the lowest and highest amounts of GN (or GO) with MAP showed XRD patterns characteristic of the commercial MAP, indicating that the presence of GN (or GO) in the mixture did not alter the structure of MAP. No diffraction peaks corresponding to either GN or GO were observed in the XDR patterns for the amended products, which is probably due to the low amounts of GN (or GO) and their diffraction intensity. However, a small decrease in the intensity of the MAP-GO composites compared to MAP could be related to the chemical reaction between MAP and GO.[44]

To confirm the presence of GN and GO in the amended MAP granules, Raman characterization was performed (Figure 2c-d). The granules showed a typical Raman spectra of GN sheets with two dominant peaks at 1346 and 1596 cm^{-1} related to the D and G bands of GN-based

materials, respectively.[45] The Raman spectrum of MAP (Figure 2c) showed a high peak at 920 cm^{-1} related to the stretching vibration of the PO_4 group and a peak at 1650 cm^{-1} which corresponds to more strongly hydrogen bonded water molecules.[46] The Raman spectrum of MAP presented in this work shows more peaks compared to the Raman spectrum of pure MAP due to the presence of some impurities such as aluminium (Al), magnesium (Mg), calcium (Ca) and sulfur (S) ions (Figure S3, Supporting Information). However, the Raman spectrum of MAP-0.05%GN showed similar peaks to the Raman spectrum of MAP, except that the intensity of the peaks were decreased and the peaks related to the D and G bands of GN were more distinct. The D and G bands of MAP-0.5%GN composite were at 1347 and 1597 cm^{-1}, respectively and were shifted compared to that of GN (used as a control) due to the charge transfer between the GN and MAP.[47] GO and its different composites with MAP followed a similar trend in Raman spectra to that of MAP-GN composites (Figure 2d). The MAP-0.5%GO composites displayed two sharp and clear peaks at 1343 (D band) and 1589 cm^{-1} (G band), similar to the peaks of GO. These results therefore confirmed the presence of GN or GO in MAP-GN and MAP-GO granules.

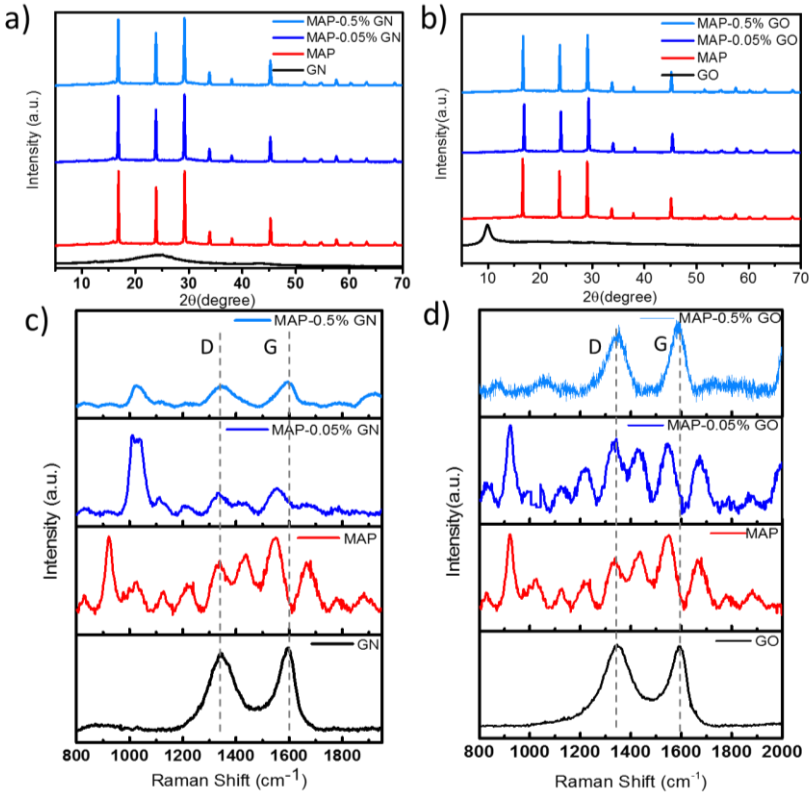

Figure 2. XRD patterns of a) graphene (GN), mono ammonium phosphate (MAP) and MAP with 0.05 and 0.5 weight percentage of GN (MAP-0.05%GN and MAP-0.5%GN), b) graphene oxide (GO), MAP and MAP with 0.05 and 0.5 weight percentage of GO (MAP-0.05%GO and MAP-0.5%GO) and Raman spectra of c) GN, MAP and MAP with 0.05 and 0.5 weight percentage of GN (MAP-0.05%GN and MAP-0.5%GN), and d) GO, MAP and MAP with 0.05 and 0.5 weight percentage of GO (MAP-0.05%GO and MAP-0.5%GO).

Physical properties

The crushing strength of MAP co-granulated with different weight percentages of GN and GO are presented in Figure 3a-d. It can be clearly observed that the crushing strength of MAP granules

with added GN (or GO) was significantly higher (3.0 to 18.2 times) than MAP (control) and the GN incorporation produced higher crushing strengths compared to GO. The average crushing strength with 0.5 wt% GN in the MAP granule was 10.8 N, which was 2.8 times higher than granules with the same amount of GO. Furthermore, increase in crushing strength of granules with GN or GO showed a non-linear concentration dependence. The average crushing strengths for GN additives showed the highest increase (10.8 N) using 0.5% GN and lowest increase (6.8 N) using 0.2% GN. The incorporation of only 0.05% GN led to a 15.5 times enhancement in the crushing strength compare to 13.5 and 11.5 times enhancement in crushing strength for granules with 0.1% and 0.2% GN added. For GO additives we observed the highest increase in crushing strength (5.0 N) with 0.5% GO added and the lowest strength (1.8 N) with 0.1% added. Adding low percentages of GN/GO showed a significant improvement in MAP granules compared to commercial additives, such as Norling A (lignosulfonate). Adding 1% of Norling A only doubled the crushing strength of MAP compared to untreated MAP.[10]

We propose that the improved crushing strength of MAP granules with GN or GO additives could be attributed to the high specific surface area and the pore-filling or interlocking ability of GMBs arising from their wrinkled and 2D (planar) structures. To support this hypothesis a series of SEM images were taken of MAP granules with GN and GO additives (Figure 3(b-f)). The rough surface of the MAP granule with many micro pores and voids (control) (Figure 3b) was significantly different to the surface of MAP with 0.5% GN added which was the most indicative evidence of the pore filling property of GN additives. The addition of GN caused a denser surface with less pores (or voids) and thus the mechanical behaviour of the granules was improved (Figure 3c). High-resolution SEM images of 0.5% MAP-GN granules revealed the presence of wrinkly GN sheets or a few layers of GN sheets between MAP macroparticles (Figures 3d-e). The same behaviour and morphological characteristics were observed for MAP granules with GO using the same concentration (Figure 3f). These results are in agreement with previous studies showing that GN and GO with lower concentrations can significantly improve the physical properties of composite materials (polymers and concrete) due to pore filling and greater interactions between the GN/GO sheets and polymer/inorganic matrix resulting from the high surface area of the planar structures of sheets.[24, 48]

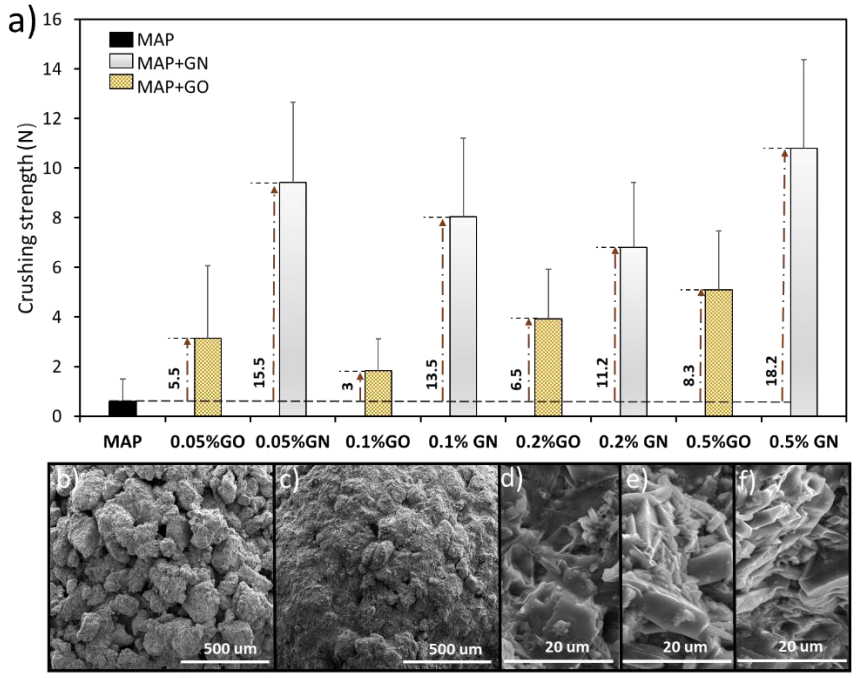

Figure 3. a) Graph showing crushing strength (N) to crush a granule of mono ammonium phosphate (MAP) (control) and MAP with different concentration (0.05 to 0.5%) of graphene (GN) and graphene oxide (GO), (crushing strength and standard deviation were measured for 25 granules for each formulation, error bars represents (n=25), Low resolution SEM images of top surface of b) MAP (control) and c) MAP-0.5%GN, high resolution SEM images of d-e) MAP-0.5%GN and f) MAP-0.5%GO

Another reason for the improved crushing strength of GN or GO-MAP granules compared to MAP could be related to the unique mechanical properties of GBMs with a high calculated Young's modulus (E) and intrinsic strength (τ_c).[20, 49, 50] The results of previous studies have shown that the measured E and τ_c was higher for GN compared to GO, and the calculated E and τ_c for GO sheets depended on the water content, thickness of the samples and presence of different functional groups on the surface of GO, as well as its OH/O ratio of oxygen functional groups.[49, 51-53] Therefore, the higher crushing strength of MAP-GN granules compared to MAP-GO granules can be attributed to the smaller value of E and τ_c of GO compared to GN. It is reported that the mechanical properties of GN are strongly influenced by the type and amount of its defects.[54] GN used in this study was prepared by hydrothermal reduction of GO, and therefore would inevitably be defective and thus inferior in properties to pristine monolayer GN, but still the E of the GN synthesized (0.25 TPa) was higher than that of GO (0.2 TPa).[55-57]

To explain the unexpected non-linear concentration dependence of GN/GO additives on the crushing strength of MAP granules showing higher crushing strength values for lower inclusion rates (0.05% GN), a schematic of their granular structures based on the SEM images of prepared MAP granules with different graphene concentrations was illustrated in Figure 4. Figure 4a explains how MAP particles agglomerate together to form granules during the granulation process. SEM

images of the MAP granules (Figure 4d-d') clearly verify the proposed schematic by showing loosely agglomerated MAP particles attached together with very rough topography of granules. Adding a low percentage of GN (0.05%) to MAP particles aided the formation of denser aggregates of MAP-GN due to the pore-filling effect of GN sheets (Figure 4b). SEM images of MAP-0.05% GN (Figure 4e-e') confirmed that the amount of pores and debris significantly decreased and MAP particles were connected tightly together due to the presence of GN showing a very smooth MAP granule surface. However, adding higher concentrations of GN (0.1%, 0.2% or 0.5%) to MAP particles during the mixing process before granulation created some initial MAP/GN aggregates due to the presence of some moisture (~20%) in the GN paste. These pre-aggregated MAP/GN particles tended to bind together and to the MAP particles during the granulation process causing the final granule to have a rougher surface compared to the MAP/GN granules with 0.05% GN (Figure 4c). SEM images of the MAP-0.1% GN granules (Figure 4f-f') showed a rougher surface with some larger aggregates compared to MAP-0.05% GN granules and the number of aggregates increased in the case of MAP-0.2% GN granules (Figure 4g-g'). Although the presence of pre-aggregated MAP/GN particles decreased the crushing strength of MAP-0.1 and 0.2% of GN/GO granules, however, their crushing strength is higher than untreated MAP granules.

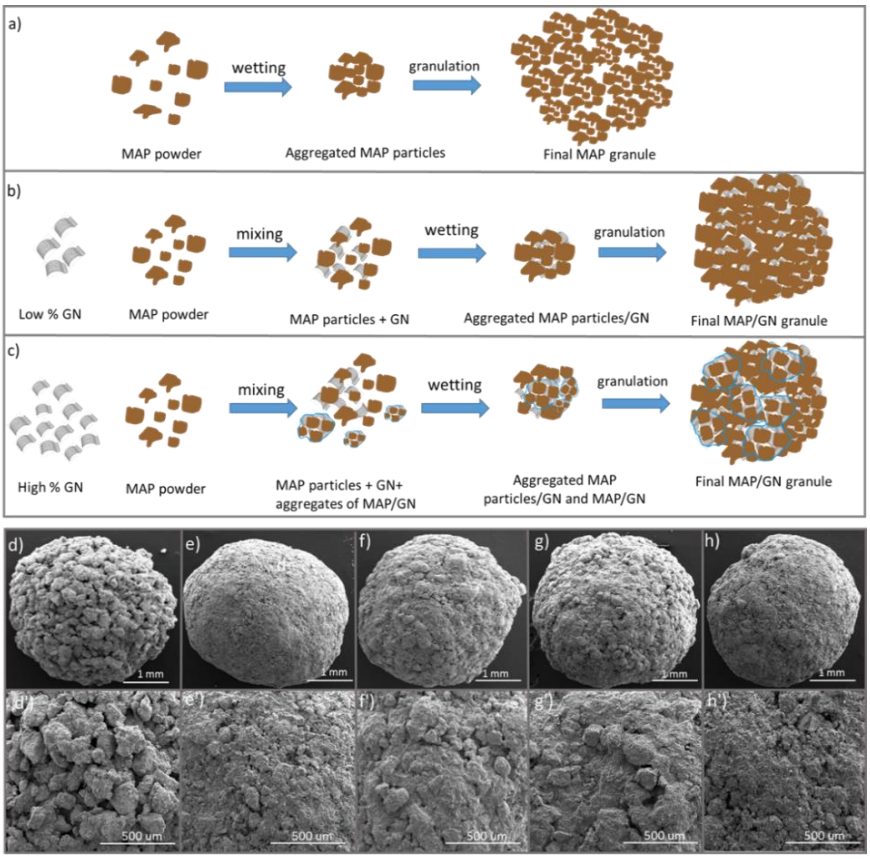

Figure 4. Schematic of co-granulation of MAP using lower and higher concentration of graphene additives a) Granulation of MAP showing "loose" connection of MAP particles during the granulation process resulting in rough and particulates surface morphology, b) Granulation of MAP with lower concentration of graphene additives (0.05% GN or GO)) showing

filling of the pores by GN or GO sheets and making smoother surface, c) Granulation of MAP with graphene additives with higher concentration (>0.1%) showing formation of pre-aggregates during the mixing process of GN and MAP, and incorporation of aggregates in the granulation process, causing more rough surface morphology. Corresponding low and high resolution SEM images of surface of d,d') mono ammonium phosphate MAP granules prepared by low and high dosages of graphene additives (MAP), and MAP with different percentages of graphene additives e,e') MAP-0.05%GN, f,f') MAP-0.1%GN, g,g') MAP-0.2%GN and h,h') MAP-0.5%GN.

Granules of MAP treated with and without GN/GO additives were dried in the oven at 50°C overnight to speed up their drying. Interestingly, the crushing strength of MAP-GO granules was considerably enhanced compared to MAP-GO granules dried at ambient temperature (Figure 5a). However, heating MAP or MAP-GN granules at 50°C did not improve their crushing strength compared to the granules dried at ambient temperature. Granules were not dried at higher temperatures to avoid changes in the crystalline structure of MAP.[58] The crushing strength of all MAP-GO formulations after heating was comparable to the MAP-GN formulations with no heating (Figure 5b). These results could be explained by the conversion of GO to reduced GO (rGO) due to heating, which is a well-known process and obviously improves the performance of GO to be similar to GN. Different characterization techniques, including FTIR, TGA, Raman and XRD were used to prove this hypothesis. Compared with other additives or coatings used to enhance the crushing strength of fertilizer granules, adding a small quantity of GN or GO sheets produced a noticeable enhancement of hardness of MAP granules, as shown in Table 1.

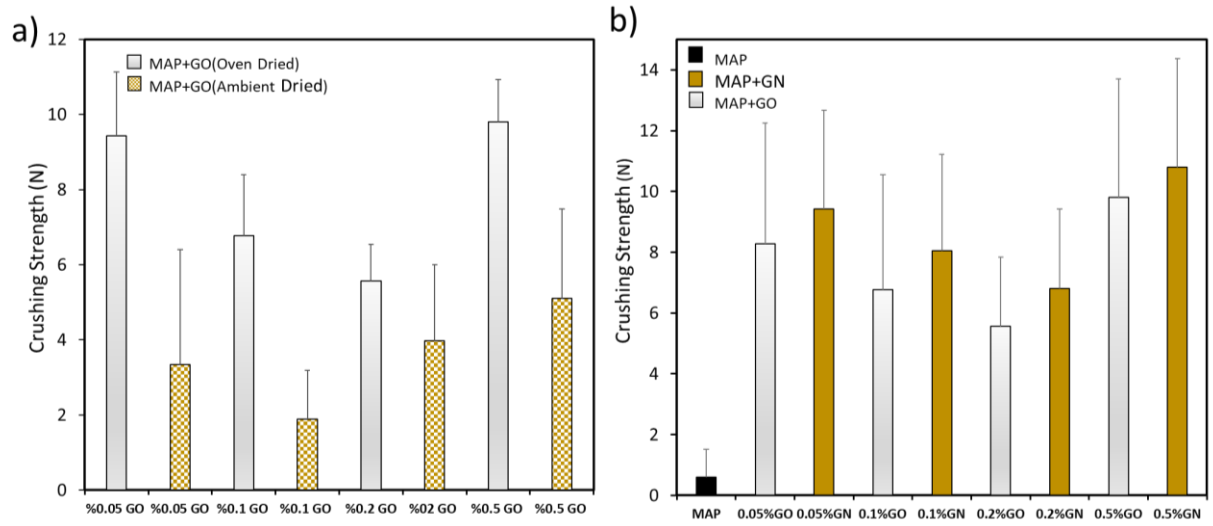

Figure 5. Comparison of crushing strength of a) Mono ammonium phosphate (MAP) mixed with different weight percentage of graphene oxide (GO) (0.05, 0.1, 0.2 and 0.5%) dried at ambient temperature and in the oven (50°C) after granulation and b) Mono ammonium phosphate mixed with different weight percentage of graphene (GN) and GO (0.05, 0.1, 0.2 and 0.5%) dried in the oven after granulation (crushing strength and standard deviation were measured for 25 granules for each formulation, error bars represents (n=25).

Table 1. Comparison of the effects of different materials used as additives or coatings to enhance the crushing strength of fertilizer granules, (a refers to reporting highest amount of crushing strength among the same fertilizer with different percentages of added or coated materials as hardening agents, b refers to composition of Norlig A product which is (3.8% calcium lignosulfonate), c refers to composition of UF85 product which is an 85% aqueous solution of urea formaldehyde, d refers to composition of clay which is a blend of diatomaceous earth and calcium bentonite, e refers to composition of Norlig HP product which is reed lignin).

Fertilizer type	Method of application	Coating or additives	Coating or additive percentage	Relative increase compare to control	Reference

Isobutyl diurea (IBDU)[a]	coating	Mixture of Norlig A [b]and urea	4.6%	1.74	[4]
(IBDU)[a]	coating	Water and urea	4.7%	1.68	[4]
(IBDU)[a]	coating	UF85[c]	6.0%	4.05	[4]
Urea	coating	Poly(butylene succinate) and Dimerized Fatty Acid	0.26%	8.09	[17]
Urea granule [a]	additive	$Ca(OH)_2$	(0.75%)	2.52	[11]
Urea granule	additive	CaO	(0.5%)	2.31	[11]
Urea granule [a]	additive	Cement	(0.1%)	1.9	[11]
Urea granule	additive	Fly Ash	(0.5%)	1.95	[11]
Urea granule [a]	additive	Clay[d] and $Ca(OH)_2$ (10/90%)	(0.6%)	2.53	[11]
Urea granule [a]	additive	Clay[d] and cement (90/10%)	(0.5)%	1.97	[11]
Urea granule [a]	additive	formaldehyde	0.6%	1.96	[11]
Ammonium nitrate [a]	additive	Norlig HP[e]	0.4%	1.48	[10]
MAP [a]	additive	lignosulfonate	0.4%	2.14	[10]
Diammonium phosphate(DAP) [a]	additive	Norlig HP[e]	0.6%	4.33	[10]
Potassium nitrate	additive	Modified lignosulfonate	5.0%	7	[10]
Potassium chloride	additive	Modified lignosulfonate	5.0%	5.75	[10]
Potassium sulfate	additive	Modified lignosulfonate	5.0%	9.8	[10]
MAP	additive	Graphene	0.5%	**18.20**	Current work
MAP	additive	Graphene	0.05%	**15.55**	Current work
MAP	additive	Graphene oxide	0.5%	**16.21**	Current work
MAP	additive	Graphene oxide	0.05%	**13.62**	Current work

The physical properties and mechanical performances of the prepared fertilizer granules were further investigated by measuring their abrasion resistance.[5] The abrasion resistance of the fertiliser granules reflects their resistance to the formation of dust and fine particles as a result of granule to granule, and granule to equipment contact when being handled and stored.[11, 40] Therefore, the abrasion resistance of MAP granules treated with different concentrations of GN was selected for the abrasion tests due to their greater mechanical strength compared to GO formulations. Figure 6a shows the abrasion percentages for MAP granules with different GN concentrations taken at 10, 20 and 30 sec from the abrasion test. Results showed that addition of GN to MAP granules significantly reduced their degradation by abrasion (>3 times) compared with untreated MAP. As expected, the degradation of the granules increased by increasing the abrasion time from 10 sec to 30 sec. Interestingly, the abrasion of MAP-GN granules was not concentration dependence and there was a negligible difference in dust formed at very low concentration of GN (0.05%) compare to higher concentration (0.5%). This could be explained by the morphological structure and surface roughness of the granules. As mentioned previously, adding 0.05% GN decreased the amount of pores and debris on the surface of MAP-0.05GN granules due to the pore-filling effect of GN sheets. However, increasing the amount of GN from 0.05% to 0.1, 0.2 and 0.5% created a rougher surface with surface aggregates compared to the smoother surface of MAP-0.05%GN granules.

Therefore, in MAP treated granules with higher concentration of GN the contacting surface between two granules, and with granules and the container increased, thus generating similar amounts of dust as 0.05% GN granules (Figure 6b). Larger aggregates on the surface of granules with high rates of added GN are more likely to separate from the granule's surface when in contact with other granules and the container during the abrasion test (Figure 6c). Furthermore, cavities developed on the surface of MAP-0.5%GN after abrasion for 30 sec was related to the detachment of surface fragments (Figure 6d).

MAP-GO samples dried under ambient conditions and in the oven were tested for abrasion resistance and the effect of longer shaking time on the abrasion of granules was studied (Figure S5, Supporting Information). The results obtained from the abrasion tests showed less dust formation for oven dried MAP-GO compared to the ambient dried MAP-GO samples. Furthermore, the abrasion of those samples with highest crushing strengths did not increase greatly with an increased shaking time of 5 min.

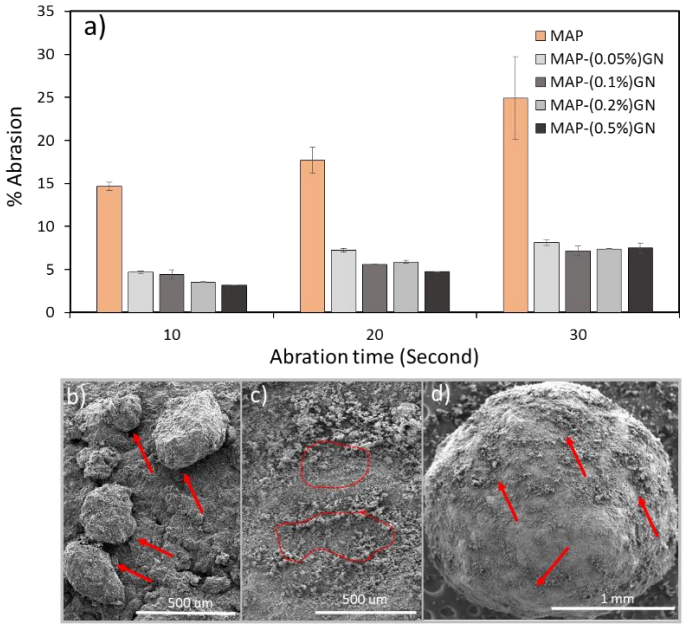

Figure 6. a) Comparative abrasion data showing degradation of pure monoammonium phosphate (MAP) granules and MAP granules prepared with different weight percentages of graphene (0.05, 0.1, 0.2 and 0.5% GN, error bars represent standard error (n=3)), SEM images of b) MAP-0.5% GN before abrasion showing aggregates on granule surface and (c and d) after abrasion for 30 seconds showing detachments of surface fragments.

Testing the impact resistance of granules is important for the fertilizer industry when (i) fan-type fertilizer spreaders are used, (ii) fertiliser granules are discharged from overhead points into a bulk piles, and (iii) bags of fertilizer products are dropped during handling.[40] The selected three formulations that showed higher crushing strength and low abrasion namely, MAP-GN with 0.05% and 0.5% addition rates of GN and oven dried MAP-GO with 0.5% GO were chosen to

conduct the impact resistance test. When the treated MAP granules were subjected to the impact resistance test, 18% of granules were fractured (Figure 7a). MAP granules co-granulated with GO and especially GN as hardening agents had much greater resistance with only 4.6% and <3% of granules fractured, respectively.

Finally, the effect of pressure and humidity on the caking tendency of MAP and selected MAP-GN/GO granules with the best physical properties was performed. For all three tested formulations (MAP, MAP-0.5% GN and MAP-0.5% GO), no caking was observed for the 1 kg load at the end of the incubation period. However, by changing the loading weight to 2.5 kg, some of the granules fractured and caking occurred as in the case of the MAP granules (Figure 7b-c). SEM images of the caked parts in the MAP granules (Figure 7d-e) shows two granules caked together and some broken granules. Both MAP-GN and MAP-GO granules flowed freely at the end of the incubation time with 2.5 kg weight load, but some MAP-GO granules were crushed under the applied pressure (Figure 7f-h). Therefore, adding a small quantity of GN or GO to MAP significantly increased the mechanical strength of granules, and consequently would reduce the amount of airborne dust created during the handling and transportation of fertilizer.

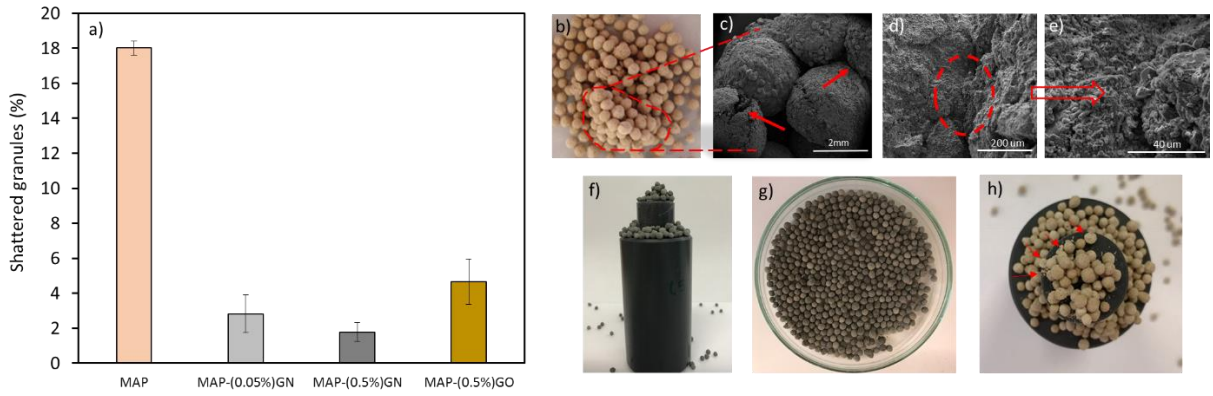

Figure 7. a) Impact resistance of pure monoammonium phosphate (MAP) granules, MAP granules treated with 0.05% graphene oxide (GO) (MAP-0.05%GO) dried in the oven, 0.05% of graphene (GN) (MAP-0.05%GN) and, 0.5% of GN (MAP-0.5%GN) (error bars represent standard error (n=3)), b) A photograph of caked monoammonium phosphate (MAP) granules under 2.5 kg weight after incubation for 1 week at 30 °C and 80% relative humidity and c-e) SEM images of caked MAP granules, f-g) Photographs of MAP treated with 0.5% of graphene and h) photograph of MAP treated with 0.5% of graphene oxide (all caking test performed three times and samples were incubated for 1 week at 30°C ,80% of humidity and under 2.5 kg of weight).

Soil diffusion experiment

As discussed previously some hardening agents or anti-caking materials added to fertilizer granules can affect the release rate of nutrients, often slowing down the release.[15-17, 59] Therefore, in this study, we investigated the diffusion and release of phosphorus (P) in the soil from MAP-GN based granules. Formulated granules (MAP-0.05%GN, MAP-0.5%GN, MAP-0.05%GO and MAP-0.5%GO) that achieved the greatest overall physical properties were selected for this experiment.

After one day application of untreated MAP with the GN/GO based treated fertilizers into the moist soil, the movement of P out of the granules and into the soil (represented by the dark green zone) from all treated MAP granules was less compared to the control MAP (Figure 8a). As can be seen from Figure 8b the diffusion of P when added with MAP-0.5%GN/GO was slightly lower compared to the soils with MAP-0.05%GN/GO. Furthermore, there was less release and diffusion of P from MAP-0.5%GO compared to MAP-0.5%GN at all incubation periods, which may be due to the chemical reaction between GO and MAP. The results from the soil diffusion test confirm that the GBMs not only increase the physical properties of MAP granules but also slightly delay the release of P.

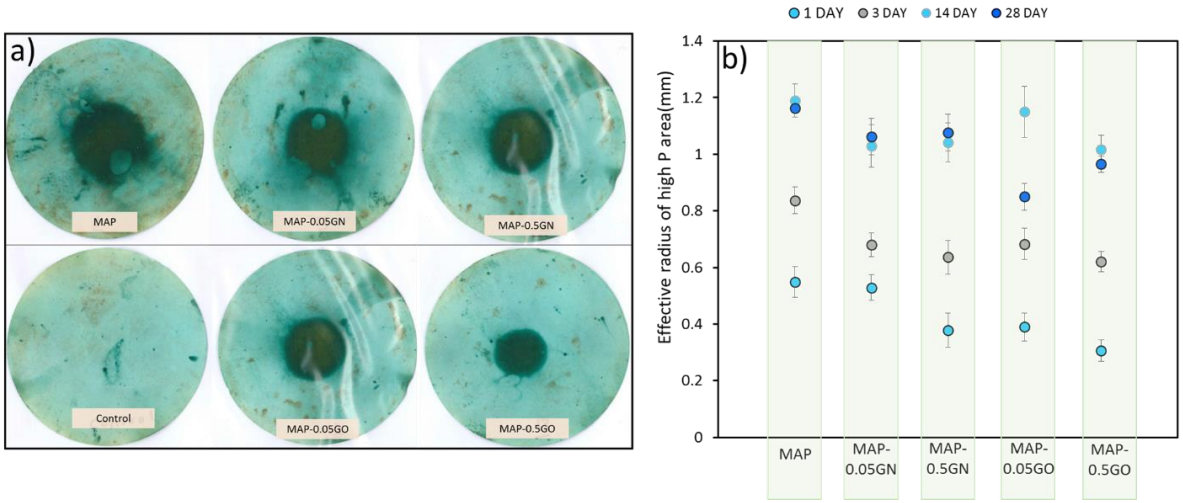

Figure 8. a) Visualized P diffusion zones in an acid soil (Monarto, Supporting Information Table S1) from monoammonium phosphate (MAP), MAP with 0.05% graphene oxide (GO) (MAP-0.05%GO), MAP-0.5%GO, MAP with 0.05% graphene (GN) (MAP-0.05%GN) and MAP-0.5%GN. All fertilizers supplied ~6.3 mg of phosphorus (P) added to soil in the centre of a Petri dish and incubated for 28 days, and b) radius of the high-P (derived as $\sqrt{A}/\pi$ with A the area of the P diffusion zone) at 1, 3, 14, 21 and 28 days after the addition of MAP, MAP-0.05%GO, MAP-0.5%GO, MAP-0.05%GN and MAP-0.5%GN granules (error bars represent standard error (n=3)).

Although the unique physio-chemical properties of GBMs has made them a favourable material for many new technologies, safety issues associated with their production, application and fate in the environment must be addressed to critically consider any future development.[60] There are a number of studies conducted to evaluate the in *vitro* and in *vivo* toxicological effects of GBMs and their interactions with different living organisms such as mammalian cells, microbes, and animal models. While most of these studies showed the biocompatibility of GBMs, some studies have indicated potential risks and health hazards. [61, 62] The toxic effects of GBMs, as for all other materials, are modular and can change depending on many parameters including the concentration, morphology, particle size and contact time, hydrophobicity, and surface functionalization.[62] Therefore it is difficult to generalize GBMs toxicity risks as these are reliant on their particular applications and require specific evaluation performed by safety organizations and standards.[63]

Another potential concern about application of GBMs in agriculture is their fate and accumulation in soils, sediments or waters. However, several recent studies have shown the biodegradation of GBMs in the presence of hydrogen peroxide (H_2O_2), horseradish peroxidase, lignin peroxidase and enzyme release by white rot fungi.[64-66] Therefore, it is anticipated that both GN and GO undergo effective biodegradation in the environment as H_2O_2 could be found naturally in rain and surface water, and fungi distributed in soil world widely.[64, 66]

CONCLUSIONS

In this work, we demonstrated for the first time that GN and GO can be used as additives in fertilizer granules to significantly improve their physical properties such as crushing strength, abrasion and impact resistance. MAP was used as a model fertilizer and GN and GO were added in the range 0.05 wt% to 0.5 wt% using a laboratory granulation process, smaller but similar to that used by fertilizer manufacturers. SEM characterization of MAP-GN and MAP-GO formulations confirmed that GN/GO sheets were randomly dispersed and embedded in the MAP co-granules improving their compactness and filled the voids between the particles. Crushing strength tests revealed that small amounts of GN (or GO) in MAP fertilizer granules remarkably increased (18.2 times for MAP-GN and 16.2 times for MAP-GO) the granule strength compared with untreated MAP. Furthermore, MAP granules containing 0.5% GN or GO abraded ~3.3 and 5 times less of the surface and produced lower dust and fines, and the mechanical tests performed showed significant impact resistance with less shattered granules (4 to 10 times) compared to control MAP. MAP-GN and GO granules also showed less or no caking when exposed to pressure and humidity. These results confirm the potential use of GN and GO as hardening agents, and anti-dusting and anti-caking additives in the fertilizer industry. Soil experiments with MAP-GN or MAP-GO granules showed a slightly slower release of P that provides an additional benefit for these additives. The granulation of GN and GO additives with fertilizer is very simple and is based on existing fertilizer granulation processes used for fertilizer manufacturing hence it could be rapidly adapted for industry applications.

Acknowledgment

The authors wish to express their appreciation for the financial support of this study by the Australian Research Council Discovery Project DP1501001760 and Project IH 150100003. Mike J. McLaughlin and Roslyn Baird acknowledge the support of The Mosaic Company LLC. The authors would like to thank Colin Rivers for assistance with co-granulation of fertilizers.

Supporting Information

Supporting information provides supplementary texts, figures, photos and tables which include, material, Characterization, XRD, Raman, TGA and FTIR peaks of GO and GN (**Figure S1**), SEM images and particle size measurement of GN and GO sheets (**Figure S2**), SEM-EDAX of untreated

MAP (**Figure S3**), FTIR, TGA, Raman and XRD characterization of oven dried and ambient dried MAP-GO granules and photos of MAP-GO ambient and oven dried (**Figure S4**), degradation of MAP-GO formulations (**Figure S5**), and **Table S1** with selected physical and chemical properties of the soil used in the soil diffusion study.

REFRENCES

1. Azeem, B.; KuShaari, K.; Man, Z. B.; Basit, A.; Thanh, T. H. Review on materials & methods to produce controlled release coated urea fertilizer. *J. Controlled Release* 2014, 181, 11-21.
2. Shaviv, A. Advances in controlled-release fertilizers. *Adv. Agron.* 2001, 71, 1-49.
3. Palacios, J. J.; Fernández-Rossier, J. *Phys. Rev. B* 2008, 77, 195428.
4. Rehberg, B. E.; Hall, W. L. Fertilizer compositions and method of making such compositions. U.S. Patent US 5238480 A: 1993.
5. Matejovic, I. Determination of carbon and nitrogen in samples of various soils by the dry combustion. *Commun. Soil Sci. Plant Anal.* 1997, 28, 1499-1511.
6. Hignett, T. P. Physical and Chemical Properties of Fertilizers and Methods for their Determination. In *Fertilizer Manual*, Hignett, T. P., Ed. Springer Netherlands: Dordrecht, 1985; pp 284-316.
7. Albadarin, A. B.; Lewis, T. D.; Walker, G. M. Granulated polyhalite fertilizer caking propensity. *Powder Technol.* 2017, 308, 193-199.
8. Bröckel, U.; Wahl, M.; Kirsch, R.; Feise, H. J. Formation and growth of crystal bridges in bulk solids. *Chem. Eng. Technol.* 2006, 29, 691-695.
9. Rutland, D. W. Fertilizer caking: Mechanisms, influential factors, and methods of prevention. *Fertilizer Res.* 1991, 30, 99-114.
10. Detroit, W. J. Lignosulfonate treated fertilizer particles. U.S. Patent US 4846871 A: 1989.
11. Aylen, P. B.; Blyth, J. C. Particulate urea with finely divided inorganic material incorporated for hardness nonfriability and anti-caking. U.S .Patent US 5782951 A: 1998.
12. Mark Stephen, R.; Tommy, C. D. Binding agents effect on physical and chemical attributes of nitrogen-fortified poultry litter and biosolids granules. 2013, 56.
13. Allan, G. G.; Freepons, D. E.; Crews, G. M. Fertilizer compositions, processes of making them and processes of using them. U.S Ptent US 4560400 A: 1985.
14. Blouin, G. M. Production of high-strength, storage-stable particulate urea. US Patent 4587358: 1986.
15. Fleming, P. S. Sulfur encapsulation of fertilizers to provide controlled dissolution rates. U.S. patent US 3576613 A: 1971.
16. Heumann, H.; Hahn, H.; Hilt, W.; Liebing, H.; Schweppe, M. Method of preparing fertilizers with retarded nutrient release. U.S. Patent US 4142885 A: 1979.
17. Lubkowski, K.; Smorowska, A.; Grzmil, B.; Kozłowska, A. Controlled-release fertilizer prepared using a biodegradable aliphatic copolyester of poly(butylene succinate) and dimerized fatty acid. *J. Agric. Food Chem.* 2015, 63, 2597-2605.
18. Mohd Ibrahim, K. R.; Eghbali Babadi, F.; Yunus, R. Comparative performance of different urea coating materials for slow release. *Particuol.* 2014, 17, 165-172.
19. Zhu, Y.; Murali, S.; Cai, W.; Li, X.; Suk, J. W.; Potts, J. R.; Ruoff, R. S. Graphene and graphene oxide: Synthesis, properties, and applications. *Adv. Mater.* 2010, 22, 3906-3924.
20. Lee, C.; Wei, X.; Kysar, J. W.; Hone, J. Measurement of the elastic properties and intrinsic strength of monolayer graphene. *Sci.* 2008, 321, 385-388.
21. Sanchez, V. C.; Jachak, A.; Hurt, R. H.; Kane, A. B. Biological interactions of graphene-family nanomaterials: An interdisciplinary review. *Chem. Res. Toxicol.* 2012, 25, 15-34.

22. Compton, O. C.; Nguyen, S. T. Graphene oxide, highly reduced graphene oxide, and graphene: versatile building blocks for carbon-based materials. *Small* 2010, 6, 711-723.
23. Potts, J. R.; Dreyer, D. R.; Bielawski, C. W.; Ruoff, R. S. Graphene-based polymer nanocomposites. *Polymer* 2011, 52, 5-25.
24. Rafiee, M. A.; Rafiee, J.; Wang, Z.; Song, H.; Yu, Z.-Z.; Koratkar, N. Enhanced mechanical properties of nanocomposites at low graphene content. *ACS Nano* 2009, 3, 3884-3890.
25. Hwang, J.; Yoon, T.; Jin, S. H.; Lee, J.; Kim, T.-S.; Hong, S. H.; Jeon, S. Enhanced mechanical properties of graphene/copper nanocomposites using a molecular-level mixing process. *Adv. Mater.* 2013, 25, 6724-6729.
26. Li, M.-X.; Xie, J.; Li, Y.-D.; Xu, H.-H. Reduced graphene oxide dispersed in copper matrix composites: Facile preparation and enhanced mechanical properties. *Phys. Status Solidi A* 2015, 212, 2154-2161.
27. Walker, L. S.; Marotto, V. R.; Rafiee, M. A.; Koratkar, N.; Corral, E. L. Toughening in graphene ceramic composites. *ACS Nano* 2011, 5, 3182-3190.
28. Kuila, T.; Bose, S.; Hong, C. E.; Uddin, M. E.; Khanra, P.; Kim, N. H.; Lee, J. H. Preparation of functionalized graphene/linear low density polyethylene composites by a solution mixing method. *Carbon* 2011, 49, 1033-1037.
29. Dreyer, D. R.; Park, S.; Bielawski, C. W.; Ruoff, R. S. The chemistry of graphene oxide. *Chem. Soc. Rev.* 2010, 39, 228-240.
30. Lv, S.; Ma, Y.; Qiu, C.; Sun, T.; Liu, J.; Zhou, Q. Effect of graphene oxide nanosheets of microstructure and mechanical properties of cement composites. *Constr. Build. Mater.* 2013, 49, 121-127.
31. Zhang, X.; An, Y.; Han, J.; Han, W.; Zhao, G.; Jin, X. Graphene nanosheet reinforced ZrB2-SiC ceramic composite by thermal reduction of graphene oxide. *RSC Adv.* 2015, 5, 47060-47065.
32. Lou, Y.; Liu, G.; Liu, S.; Shen, J.; Jin, W. A facile way to prepare ceramic-supported graphene oxide composite membrane via silane-graft modification. *Appl. Surf. Sci.* 2014, 307, 631-637.
33. Chuah, S.; Pan, Z.; Sanjayan, J. G.; Wang, C. M.; Duan, W. H. Nano reinforced cement and concrete composites and new perspective from graphene oxide. *Constr. Build. Mater.* 2014, 73, 113-124.
34. Sharma, S.; Kothiyal, N. C. Influence of graphene oxide as dispersed phase in cement mortar matrix in defining the crystal patterns of cement hydrates and its effect on mechanical, microstructural and crystallization properties. *RSC Adv.* 2015, 5, 52642-52657.
35. Wang, B.; Jiang, R.; Wu, Z. Investigation of the mechanical properties and microstructure of graphene nanoplatelet-cement composite. *Nanomater.* 2016, 6, 200.
36. Qin, H.; Wei, W.; Hang Hu, Y. Synergistic effect of graphene-oxide-doping and microwave-curing on mechanical strength of cement. *J. Phys. Chem. Solids* 2017, 103, 67-72.
37. Pan, Z.; He, L.; Qiu, L.; Korayem, A. H.; Li, G.; Zhu, J. W.; Collins, F.; Li, D.; Duan, W. H.; Wang, M. C. Mechanical properties and microstructure of a graphene oxide–cement composite. *Cem. Concr. Compos.* 2015, 58, 140-147.
38. Marcano, D. C.; Kosynkin, D. V.; Berlin, J. M.; Sinitskii, A.; Sun, Z.; Slesarev, A.; Alemany, L. B.; Lu, W.; Tour, J. M. Improved synthesis of graphene oxide. *ACS Nano* 2010, 4, 4806-4814.
39. Zhou, Y.; Bao, Q.; Tang, L. A. L.; Zhong, Y.; Loh, K. P. Hydrothermal dehydration for the "Green" reduction of exfoliated graphene oxide to graphene and demonstration of tunable optical limiting properties. *Chem. Mater.* 2009, 21, 2950-2956.
40. *Fertilizer manual / editors, United Nations Industrial Development Organization (UNIDO) and International Fertilizer Development Center (IFDC)*. Kluwer Academic Publishers : Sold and distributed by IFDC: Dordrecht, The Netherlands : Muscle Shoals, AL, 1998.
41. Lafci, A.; Gürüz, K.; Yücel, H. Investigation of factors affecting caking tendency of calcium ammonium nitrate fertilizer and coating experiments. *Fertilizer Res.* 1988, 18, 63-70.
42. Degryse, F.; McLaughlin, M. J. Phosphorus diffusion from fertilizer: visualization, chemical measurements, and modeling. *Soil Sci. Soc. Am. J.* 2014, 78, 832-842.

43. Moon, I. K.; Lee, J.; Ruoff, R. S.; Lee, H. Reduced graphene oxide by chemical graphitization. *Nat. Commun.* 2010, 1, 73.
44. Salavagione, H. J.; Martinez, G.; Gomez, M. A. Synthesis of poly(vinyl alcohol)/reduced graphite oxide nanocomposites with improved thermal and electrical properties. *J. Mater. Chem.* 2009, 19, 5027-5032.
45. Tran, D. N. H.; Kabiri, S.; Losic, D. A green approach for the reduction of graphene oxide nanosheets using non-aromatic amino acids. *Carbon* 2014, 76, 193-202.
46. Frost, R. L.; Scholz, R.; López, A.; Xi, Y. A vibrational spectroscopic study of the phosphate mineral whiteite CaMn++Mg2Al2(PO4)4(OH)2·8(H2O). *Spectrochim. Acta Part A: Mol. Biomol. Spectrosc.* 2014, 124, 243-248.
47. Kabiri, S.; Tran, D. N. H.; Cole, M. A.; Losic, D. Functionalized three-dimensional (3D) graphene composite for high efficiency removal of mercury. *Environ. Sci.: Water Res. Technol.* 2016, 2, 390-402.
48. Lu, Z.; Hou, D.; Meng, L.; Sun, G.; Lu, C.; Li, Z. Mechanism of cement paste reinforced by graphene oxide/carbon nanotubes composites with enhanced mechanical properties. *RSC Adv.* 2015, 5, 100598-100605.
49. Liu, L.; Zhang, J.; Zhao, J.; Liu, F. Mechanical properties of graphene oxides. *Nanoscale* 2012, 4, 5910-5916.
50. Chen, C.; Rosenblatt, S.; Bolotin, K. I.; Kalb, W.; Kim, P.; Kymissis, I.; Stormer, H. L.; Heinz, T. F.; Hone, J. Performance of monolayer graphene nanomechanical resonators with electrical readout. *Nat. Nano* 2009, 4, 861-867.
51. Dikin, D. A.; Stankovich, S.; Zimney, E. J.; Piner, R. D.; Dommett, G. H. B.; Evmenenko, G.; Nguyen, S. T.; Ruoff, R. S. Preparation and characterization of graphene oxide paper. *Nature* 2007, 448, 457-460.
52. Chen, H.; Müller, M. B.; Gilmore, K. J.; Wallace, G. G.; Li, D. Mechanically strong, electrically conductive, and biocompatible graphene paper. *Adv. Mater.* 2008, 20, 3557-3561.
53. Chen, C.; Yang, Q.-H.; Yang, Y.; Lv, W.; Wen, Y.; Hou, P.-X.; Wang, M.; Cheng, H.-M. Self-assembled free-standing graphite oxide membrane. *Adv. Mater.* 2009, 21, 3007-3011.
54. Zandiatashbar, A.; Lee, G.-H.; An, S. J.; Lee, S.; Mathew, N.; Terrones, M.; Hayashi, T.; Picu, C. R.; Hone, J.; Koratkar, N. Effect of defects on the intrinsic strength and stiffness of graphene. *Nat. Commun.* 2014, 5, 3186.
55. Suk, J. W.; Piner, R. D.; An, J.; Ruoff, R. S. Mechanical properties of monolayer graphene oxide. *ACS Nano* 2010, 4, 6557-6564.
56. Park, S.; Ruoff, R. S. Chemical methods for the production of graphenes. *Nat. Nano* 2009, 4, 217-224.
57. Perreault, F.; Fonseca de Faria, A.; Elimelech, M. Environmental applications of graphene-based nanomaterials. *Chem. Soc. Rev.* 2015, 44, 5861-5896.
58. Hikita, T.; Chubachi, Y.; Ikeda, T. X-Ray Study of the phase transition in $K_2Mn_2(SO_4)_3$. *J. Phys. Soc. Japan* 1978, 44, 525-528.
59. Wittenbrook, L. S.; Scheiderer, E. L. Coated controlled-release product. U.S. Patent US 4082533 A: 1978.
60. Ferrari, A. C.; Bonaccorso, F.; Fal'ko, V.; Novoselov, K. S.; Roche, S.; Boggild, P.; Borini, S.; Koppens, F. H. L.; Palermo, V.; Pugno, N.; Garrido, J. A.; Sordan, R.; Bianco, A.; Ballerini, L.; Prato, M.; Lidorikis, E.; Kivioja, J.; Marinelli, C.; Ryhanen, T.; Morpurgo, A.; Coleman, J. N.; Nicolosi, V.; Colombo, L.; Fert, A.; Garcia-Hernandez, M.; Bachtold, A.; Schneider, G. F.; Guinea, F.; Dekker, C.; Barbone, M.; Sun, Z.; Galiotis, C.; Grigorenko, A. N.; Konstantatos, G.; Kis, A.; Katsnelson, M.; Vandersypen, L.; Loiseau, A.; Morandi, V.; Neumaier, D.; Treossi, E.; Pellegrini, V.; Polini, M.; Tredicucci, A.; Williams, G. M.; Hee Hong, B.; Ahn, J.-H.; Min Kim, J.; Zirath, H.; van Wees, B. J.; van der Zant, H.; Occhipinti, L.; Di Matteo, A.; Kinloch, I. A.; Seyller, T.; Quesnel, E.; Feng, X.; Teo, K.; Rupesinghe, N.; Hakonen, P.; Neil, S. R. T.; Tannock, Q.; Lofwander, T.; Kinaret, J. Science and technology roadmap for graphene, related two-dimensional crystals, and hybrid systems. *Nanoscale* 2015, 7, 4598-4810.

61. Montagner, A.; Bosi, S.; Tenori, E.; Bidussi, M.; Alshatwi, A. A.; Tretiach, M.; Prato, M.; Syrgiannis, Z. Ecotoxicological effects of graphene-based materials. *2D Mater.* 2017, 4, 012001.
62. Lalwani, G.; D'Agati, M.; Khan, A. M.; Sitharaman, B. Toxicology of graphene-based nanomaterials. *Adv. Drug Delivery Rev.* 2016, 105, 109-144.
63. Bianco, A. Graphene: Safe or toxic? The two faces of the medal. *Angewandte Chem., Int. Ed.* 2013, 52, 4986-4997.
64. Lalwani, G.; Xing, W.; Sitharaman, B. Enzymatic degradation of oxidized and reduced graphene nanoribbons by Lignin Peroxidase. *J. Mater. Chem. B, Mater. for Biol. Med.* 2014, 2, 6354-6362.
65. Kotchey, G. P.; Zhao, Y.; Kagan, V. E.; Star, A. Peroxidase-mediated biodegradation of carbon nanotubes in vitro and in vivo. *Adv. Drug Delivery Rev.* 2013, 65.
66. Xing, W.; Lalwani, G.; Rusakova, I.; Sitharaman, B. Degradation of graphene by hydrogen peroxide. *Part. Part. Syst. Char.* 2014, 31, 745-750.